PERGAMON

Journal of Structural Geology 22 (2000) 1855–1873

JOURNAL OF STRUCTURAL GEOLOGY

www.elsevier.nl/locate/jstrugeo

The emplacement of the Rieserferner Pluton (Eastern Alps, Tyrol): constraints from field observations, magnetic fabrics and microstructures

A. Steenken*, S. Siegesmund, T. Heinrichs

Institut für Geologie und Dynamik der Lithosphäre—University of Göttingen, Goldschmidstr.3, D-37077 Göttingen, Germany

Received 17 November 1999; accepted 24 May 2000

Abstract

Within the alpine chain several Tertiary intrusions (e.g. Bergell, Adamello) intruded along the Periadriatic Lineament. This study attempts to show how the Rieserferner Pluton (Vedrette di Ries) is related to the Defereggen-Antholz-Vals (DAV)-Line. For a survey of the fabric pattern over the pluton the anisotropy of the magnetic susceptibility (AMS) was determined on nearly 170 samples. Low bulk susceptibilities of $K_{vol} < 450 \times 10^{-6}$ SI and a total degree of anisotropy $P' < 1.2$ point to a paramagnetic control of the magnetic properties. The coincidence between the magnetic fabric and the macroscopic fabric was proven via texture measurements and the HFA technique. Within the western Rieserferner Pluton microstructures gave no evidence for a solid-state deformation of the plutonic rocks while the central domain presents a continuum from magmatic structures in the south to a penetrative solid-state deformation along the northern margin. Structural observations indicate that the magma was locally emplaced along an active strike-slip fault. The magnetic foliation of the pluton forms three interconnected asymmetric dome structures corresponding to the Western, Central and Eastern Rieserferner. Generally, E–W-trending lineations are sigmoidally deflected along the northern and southern contact of the Central Rieserferner. Weakly defined fabrics in the Western Rieserferner suggest magma accommodation in some kind of pull apart structure related to the left lateral shear on the DAV-Line. In the Central Rieserferner preferred orientation of contact metamorphic sillimanite as well as syn-intrusive isoclinal folds indicate the thinning of the partly preserved roof envelope of the pluton, implying some ballooning of the topmost intrusion during the final stage of emplacement.

1. Introduction

The evolution of a silicic magma begins with the segregation of melt caused by thermal anomalies in the upper mantle or deeper crust. The ascent of these melts leads to the emplacement of large magmatic bodies within higher crustal levels. During cooling, minerals start to crystallise and strain conditions can be recorded by deformation features. A continuous change of the proportion between melt and crystals, as well as the specific response of the various crystallised phases to deformation could reflect the whole range from true magmatic fabrics to low-temperature solid-state fabrics. The intensity of fabrics in magmatic rocks is often less than in other common rock types. Nevertheless the significance of orientation and shape of crystals due to flattening or constrictional strain is the same. A careful description and measurement of these fabrics in a magmatic rock therefore might be able to provide important information on the emplacement mechanism, which is closely related to the 'space-problem' of granite tectonics. However the reconstruction of the time/temperature/deformation history of the magma is handicapped since we can not determine the time when fabrics start to develop. In the early stages of crystallisation only a few crystal grains are freely rotating in a melt and the capture of these fabrics is hardly possible. Therefore the development of magmatic fabrics is restricted to a late stage of solidification (Paterson et al., 1998). Whether fabrics of a pluton could reflect strain conditions during emplacement in that way is largely dependent on the speed of emplacement and cooling of the melt.

As for the relationship between the pluton and the surrounding country rocks, a large number of different emplacement styles are to be considered. They range from passive emplacement models, like stoping (Daly, 1933; Pitcher, 1970), to forceful mechanisms of magmatic wedging (Pitcher and Read, 1959), and expansion models (Ramsey, 1989) including ballooning (Holder, 1979). Contrary to the former view of Buddington (1959), that different emplacement styles are dependant on the rheological behaviour of the crust, Pitcher and Berger (1972) and

* Corresponding author.

E-mail addresses: asteenk@gwdg.de (A. Steenken), ssieges@gwdg.de (S. Siegesmund), theinri@gwdg.de (T. Heinrichs).

0191-8141/00/$ - see front matter
PII: S0191-8141(00)00071-7

Hutton (1982) reported a series of active and passive emplacement styles for the Main Donegal Granite (Ireland) at actually the same crustal level.

Recent investigations on granite tectonics put emphasis on the regional setting of plutons with respect to fault zones, which were active during magma emplacement (Hutton and Reavy, 1992), as well as on the orientation and the shape of plutons (Brun et al., 1990, Gleizes et al., 1998). So-called syn-tectonic plutons might reflect different kinds of fabrics responding in part to the internal forces and partly to the regional kinematics during cooling and solidification of magma (Hutton, 1988). As it turns out such differentiation seems to be insignificant, because resulting fabrics in plutons are due to the interaction of the buoyancy of the ascending magma and the regional strain field (Saint Blanquat and Tikoff, 1997).

In this paper we will document the regional orientation and distribution of fabrics within the Tertiary Rieserferner Pluton (Vedrette di Ries) and its country rocks and the relation to the kinematics along the Oligocene Defereggen-Antholz-Vals (DAV)-Line. The pronounced elongate shape coupled with the preservation of large parts of the psammopelitic roof give the Rieserferner Pluton a unique position among the 'Periadriatic Intrusions' in the Alps. On the basis of its two-dimensional appearance in map-view, the main body comprises a western and central part (Western and Central Rieserferner, respectively). The elongate, generally only some 100 m wide, tail exposed along the Defereggen Valley is referred to as the Eastern Rieserferner.

For the determination of fabric orientation within the intrusive rocks of the Rieserferner Pluton the anisotropy of magnetic susceptibility (AMS) was measured. Texture measurement of the biotite fabric as well as the determination of macroscopic structure and of enclave-ratios in the field was used to constrain the significance of the magnetic data. Furthermore a detailed microstructural description of the intrusive rocks provides information whether fabrics are related to magmatic, submagmatic or solid-state deformation. Since AMS-fabric and macroscopic fabrics show a tight correspondence, magnetic axes are taken to represent the directional fabric within the Rieserferner Pluton.

2. Geological background

The Oligocene Rieserferner Pluton is an elongate intrusion about 40 km long and 7 km wide, within the Austroalpine basement of the eastern Alps. It belongs to the series of the Tertiary so-called 'Periadriatic Intrusions', like the plutons of Adamello and Bergell, emplaced along the boundary between the southern and central Alps (Rosenberg et al., 1995; John and Blundy, 1993) (Fig. 1). The remarkably elongate shape of the Rieserferner Pluton differs from the typical circular outlines of many 'Periadriatic Intrusions'.

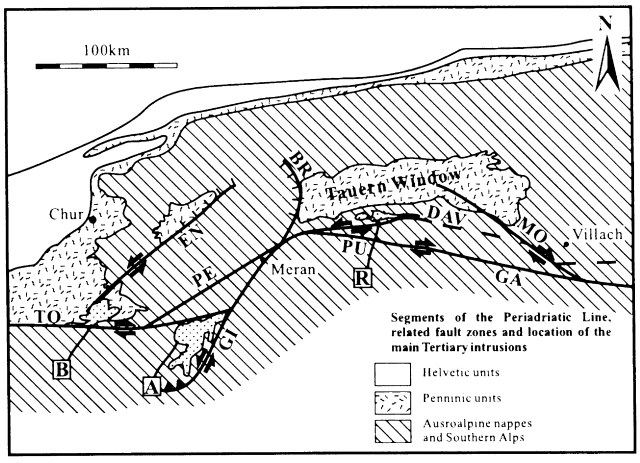

Fig. 1. Schematic map of the segments of the Periadriatic Line and related Alpine faults. (from W to E: TO—Tonale, GI—Giudicarie, PE—Pejo, BR—Brenner, PU—Puster Valley, DAV—Defereggen-Antholz-Vals, GA—Gail Valley, MO—Möll Valley). B, A and R refer to the major 'Periadriatic Intrusions' Bergell, Adamello and Rieserferner, respectively (modified after Schmid et al., 1989).

The origin of the melts of these intrusions has been controversial for a long time. The andesitic calc-alkaline character of the magmas was generally assumed to denote late-stage subduction-related magmatism during the Upper Eocene (Sassi et al., 1980). Geochemical findings (Bellieni et al., 1981) or more recently Kagami et al. (1991) support this interpretation. Other models in this debate are extension-related melting (Laubscher, 1983) or the melting of the crustal mountain root following convective thinning of the alpine lithospheric root (Dewey, 1988). Von Blanckenburg and Davis (1995, 1996) introduced the slab break-off hypothesis as a consequence of the isotopic composition and the regional distribution of the plutons along the Periadriatic fault system. Nearly all of them intruded to the north of the Periadriatic Line (PL) or a related simultaneously active fault system, such as the DAV-Line.

Kleinschrodt (1978) reported a sinistral character of the DAV-Line based on quartz fabrics of the mylonites. It divides the Austroalpine basement between the Tauern Window and the Puster-Valley-Line into parts of different cooling histories. For the kinematics of the sinistral DAV-Line, and the opposing dextral Puster-Valley-Line, a lateral escape of the block in the middle was suggested by Schmid et al. (1989). More recently the 'lateral escapement model' was forwarded by Ratschbacher et al. (1991). The eastern part of the Rieserferner Pluton is directly bordered to the south by the DAV-Line (Fig. 5). To the west the fault bends to the WSW, where the small, elongate Zinsnock Pluton crops out in between the DAV-Line and the Rieserferner Pluton. The southern border of the Zinsnock Pluton is close the DAV-Line. A synclinal fold within the Austroalpine basement separates both intrusives. The relationship between these two intrusives is still uncertain. Mager (1985) concluded from the slight dip of the contact aureole

that both plutons are connected to some extent below the surface. Bellieni (1980) drew attention to the geochemical differences between the magmas and deduced that the Austroalpine basement to the north of the DAV-Line was invaded by numerous individual granitoid melts which rose up along fault zones, and were concentrated respectively in the Zinsnock and Rieserferner Pluton. Besides, these melts may be liable for a number of smaller intrusions to the north of the DAV-Line, like the Rensenspitze and Altenberg (Monte Alto) (Bellieni et al., 1984).

Vertical movements across the DAV-Line are restricted to the Oligocene (35 Ma) basing interpretation solely on K/Ar–, as well as Rb/Sr–mica cooling ages (Borsi et al., 1973, 1978; Stöckhert, 1984). Zircon fission track ages (Stöckhert et al., 1999) indicate that this activity continued until 22 Ma. A vertical displacement of at least 200 m indicated by apatit fission track ages was determined by Coyle (1994), while Grundmann and Morteani (1985) found no further vertical displacement until 10 Ma. Elevation of the crustal block to the north of the DAV-Line exposes a partial alpine greenschist facies metamorphic overprint of variscan amphibolite facies mineral associations and structures. They are juxtaposed to the variscan structures and metamorphic associations retained to the south of the line (Stöckhert, 1982; Schönhofer, 1999). Borsi et al. (1979) determined a Rb/Sr whole rock isochron of 30 ± 3 Ma, which is the best available approximation for the intrusion age of the Rieserferner Pluton.

The lithological composition of the Rieserferner Pluton ranges from dioritic to granitic, with predominance of tonalitic to granodioritic rocks (Bellieni, 1976). The primary modal composition consists mainly of plagioclase (40–50%), quartz (10–25%), K-feldspar (5–10%), biotite (10–20%) and hornblende (0–10%). Also in some areas of the western part of the pluton magmatic garnets occur. At least four subparallel fractionation trends of Rb and Sr within these variably differentiated magmas were interpreted to reflect different crustal sources of anatexis and/or different degrees in crustal contamination (Bellieni, 1978). Furthermore high $^{87}Sr/^{86}Sr$-initial ratios of the Rieserferner Pluton indicate a crustal contamination (Borsi et al., 1979). With the exception of the garnet-bearing tonalites in the western part, none of the magma variations were traced in the field. On the base of differently fractionated REE's Bellieni et al. (1981) set up a model of two-stage fractional crystallisation explaining the geochemical variability of the pluton. They concluded that strongly fractionated H-REE-patterns ($(Tb/Yb)_N > 1$) were created during a first high pressure fractionation with the separation of garnet and amphibole, while during the second stage precipitation of amphibole and plagioclase produced low $(Tb/Yb)_N$-ratios ($(Tb/Yb)_N < 1$).

The intrusion depth of the pluton was inferred from contact metamorphism by Cesare (1992) observing a prograde metamorphic sequence. The peak of this sequence is characterised by the second sillimanite isograd pointing to at least 2.9 kbar, corresponding to a depth of 9 km and to 600–620°C on the contact. A linear interpolation between the temperature and time of the intrusion and the Rb/Sr biotite ages in the country rocks outside the contact aureole implies a basement temperature of 400–450°C during the intrusion.

Structures within the Rieserferner Pluton are directly related to the cooling of the magma and a simultaneous syn-tectonic overprint due to the movements along the DAV-Line (Steenken et al., 1999). Mann and Scheuvens (1998) found evidence for a submagmatic deformation followed by a solid-state deformation under greenschist facies conditions. Henry (1975) detected, via AMS measurements, a well-defined lineation in the Rieserferner Pluton. In accordance with structural aspects this lineation should be related to a late alpine E-W-directed compression of the pluton.

3. Field observations

3.1. Petrologic subunits of the pluton, late-stage intrusions, enclaves and their relation to macroscopic fabric

The Rieserferner Pluton is an E-W-trending predominantly tonalitic to granodioritic intrusive complex surrounded by greenschist facies metapelitic to psammopelitic rocks of the Austroalpine basement. Outcrop conditions in the main body of the pluton are excellent, except for some block fields and recent glaciers. Along the Defereggen-Valley quaternary, sediments cover large parts of the pluton and outcrops are restricted to some cliffs and small creeks. The exposed vertical relief of the main body is up to 2000 m, permitting a near-perfect 3-D reconstruction of the fabrics and providing a fair amount of information on the original shape of the pluton. The transition between the Western and Central Rieserferner is almost totally hidden below metapelitic to psammopelitic country rock that represents a portion of nearly completely preserved roof envelope. The roof reveals a vaulted shape of the Central Rieserferner implying a structural limit between the two parts of the pluton. Also some of the most elevated regions of the pluton are still topped by isolated remnants of the metasedimentary roof.

A striking feature of the magmatic rocks of the pluton is the variability in grain size (Fig. 2a). Along the western and north-western periphery coarse-grained granitoids with plagioclases and biotite-piles up to 0.8 cm in diameter occur, wedging out along the northern border of the Central Rieserferner (Fig. 5). In contrast, the main constituents of the whole body are medium- to fine-grained and of predominantly granodioritic to granitic compositions with an average grain size of 0.3 cm. A common characteristic of the coarse-grained granitoids is the appearance of magmatic garnets (Bellieni et al., 1979). They are up to 4 cm in diameter and generally exhibit a mafic decomposition rim. The frequency of these garnets increases towards the more

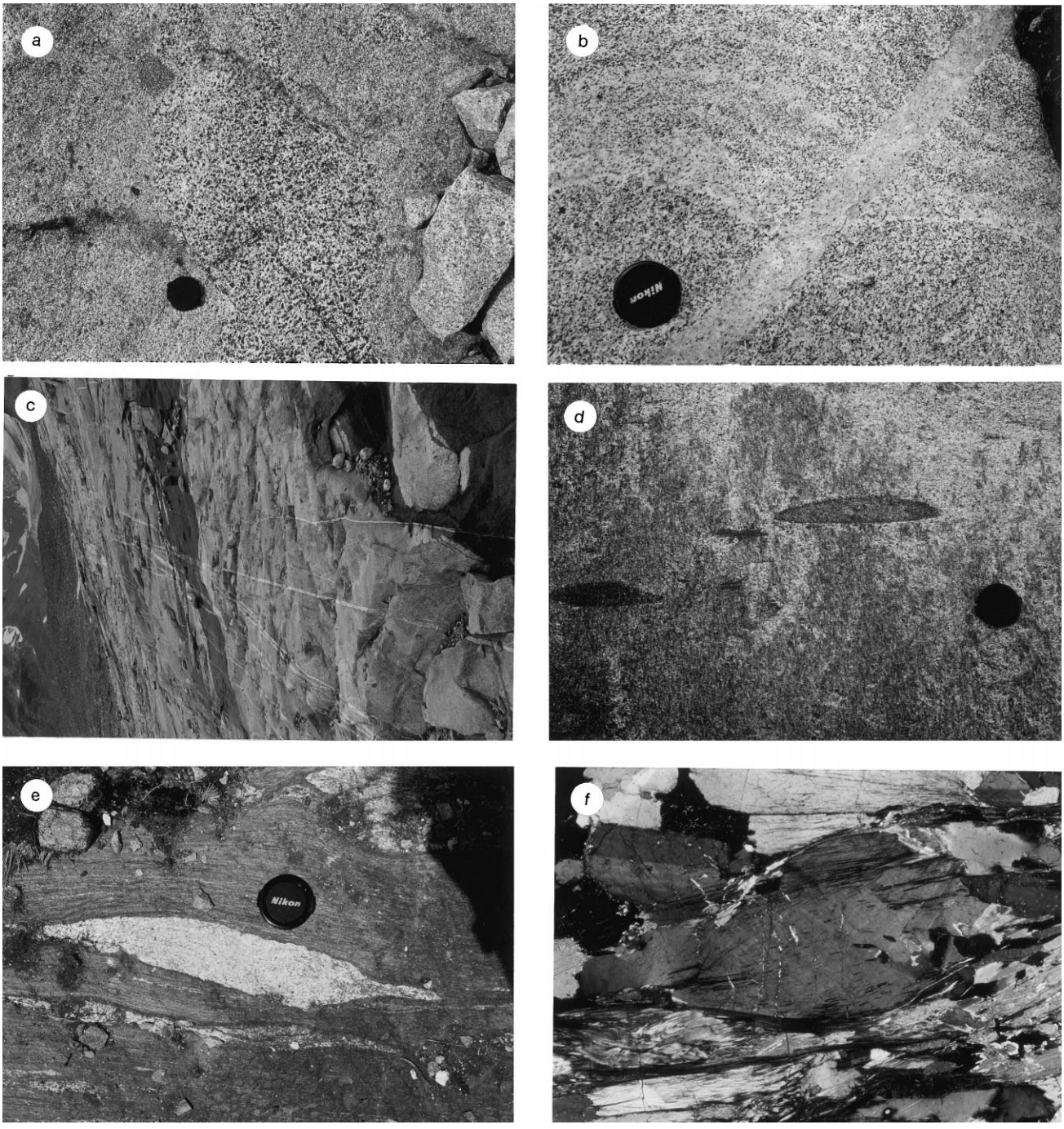

Fig. 2. (a) Tall enclave of coarse-grained tonalite within the fine-grained granodiorite at the western margin of the Central Rieserferner (for scale: black camera lid is 5 cm in diameter). (b) Characteristic 'schlieren' layering observed in some parts of the 'mafic' fine-grained granodiorites. Light bands are rich in quartz, plagioclase and biotite, whereas in the mafic layers amphibole becomes important also. The weakly developed magmatic foliation parallels the leucocratic aplitic dike (from the lower left to the upper right) crosscutting the layering (for scale see above). (c) Subparallel aplitic dikes in the Central Rieserferner can be traced for some hundred meters. Weakly oblique dykes belong to the same generation indicated by magmatic contacts between the different dykes. (d) Microgranular enclaves in a rock face almost vertical to the macroscopic y–z-plane. The 3D reconstruction will reveal the oblate shape of the enclave. (e) Boudinaged melt injection within the mylonites along the northern contact of the Central Rieserferner (for scale see above). (f) Textured growth of contact metamorphic sillimanite within the metapelitic country rock of the western border of the Central Rieserferner (width of view 1.2 mm, CPL).

tonalitic compositions of the magma. The amphibole content within these rocks is up to 10%. The amphiboles are stubby shaped with long axes up to 1.5 cm. Some exhibit a macroscopically visible biotite core. Up to 3-mm black shiny needles of allanite can be noticed almost everywhere in the pluton.

Within the large body of medium- to fine-grained granodiorites two different magma types can be distinguished by

petrological data. (i) A relatively 'mafic', mainly biotite-bearing granodioritic-to-granitic batch, which frequently exhibits a characteristic schlieren layering (Fig. 2b). Accessory amphiboles may reach a size of up to 1 cm in diameter. They are unevenly distributed within the granodiorites and probably represent an early-crystallised phase that was transported within the ascending magma. (ii) A leucocratic predominantly granodioritic magma. In some places up to 3 cm long K-feldspar megacrysts were observed, which take on a shape-preferred orientation, parallel to the biotite foliation. These megacrysts show numerous macroscopically visible inclusions of biotite and plagioclase. Amphibole is hardly noticed in this subunit. A few outcrops exhibit a sharp boundary between these two sub units. The difference between these two magma types is due to different fractionation trends as inferred from geochemical data (Bellieni et al., 1981). Furthermore, the geochemical data indicate that different melts constitute the 'mafic' granodiorites, in particular the occurrence of tonalitic melts at the transition towards the coarse-grained granitoids of the western periphery (Bellieni, 1978).

The transition between the coarse-grained tonalitic to granitic varieties of the western periphery and the inward following medium- to fine-grained granitoids is a few hundred meters wide. It is characterised by an alternation of coarse- and medium-grained rocks with intermediate compositions in between. Sharp boundaries are hardly observed, except for some large enclaves of coarse-grained tonalites along the western border of the Central Rieserferner (Fig. 2a). This transition may point to a fast intrusion sequence with an intensive mixing of the two melts, while enclaves of coarse-grained tonalites probably sank inside the crystal mush of the finer-grained granodiorite. Minor occurrences of quartz dioritic magmas are restricted to some marginal areas along the Eastern Rieserferner. These are characterised by high modal contents of biotite and amphibole. Also garnets with up to 0.5 cm in diameter can be noticed.

The intrusive rocks of the Rieserferner Pluton exhibit a well-defined macroscopic planar and/or linear fabric by the arrangement of tabular-shaped crystals (biotite and plagioclase), except for some locations on the western periphery where fabrics are hard to recognise. Fabrics cut internal contacts between the main intrusive units, and moreover the foliation within the aplitic veins parallels the foliation in the host. Therefore, the foliation postdates the intrusive juxtaposition of the compositional types.

Late-stage intrusive rocks are aplitic and pegmatitic veins as well as lamprophyre dykes. Aplites and pegmatites generally strike ENE–WSW with an inclination towards the central axis of the pluton. They are from 1 cm up to 2 m wide and exhibit a magmatic contact towards the host. On glacier-polished surfaces these veins and smaller dykes could be traced for some hundred meters (Fig. 2c). They are subparallel to each other and vary only slightly in thickness. However, some aplites crosscut the generally subparallel swarms at a low angle, but the crosscutting relationships nevertheless indicate that these dykes intruded simultaneously. Differences in grain size were not observed, even in the thickest dykes. In some places an offset of a few centimetres across the veins, indicated by disconnected microgranular enclaves, is obvious. Within the country rock aplitic to pegmatitic melts related to the Rieserferner Pluton are rarely noticed.

Lamprophyre dykes are less frequent than the aplites and pegmatites. They are vertical, have a wide variability in strike around NW–SE and commonly continue into the country rocks. Their thickness ranges from a few centimetres up to several meters. Sharp contact relationships to the host and intersected aplites and pegmatites indicate them as the latest successors in the intrusion history. A biotite K–Ar age determination of these lamprophyre dykes yields an age of 26.3 (+ 0.7 Ma), clearly post-intrusive and therefore setting an upper limit for syn-intrusive deformation. The wider dykes developed a chilled margin. Foliated sharp-edged fragments of granodiorite within the lamprophyre melt are frequently observed. In some places the piercing of tiny discontinuous lamprophyric apophyses along small fractures within the granodiorite can be observed. A conspicuous feature of the wide lamprophyre dykes is the fracturing of an already solidified melt by the injection of a second slightly more leucocratic melt. Microstructures of these dykes within the pluton and in the country rock exhibit pure magmatic structures, except some retrograde replacement of biotite by chlorite.

Using the strike of dykes as a proxy to the regional compression direction, Schulz (1994) concluded a rotation of σ_1 of the stress-field from NE–SW to NW–SE with the intrusion proceeding. This correlates with a change from sinistral transpressive movements along the DAV-Line to a dextral strike slip offset along the Puster-Valley-Line (Heinisch and Sprenger, 1988, Schulz, 1989). In this context the occurrence of several N–S to NE–SW striking brittle faults with a sinistral displacement could be explained in terms of antithetic riedel-shears related to the Puster-Valley-Line (see also Schönhofer, 1999).

At least two groups of xenolithic inclusions within the Rieserferner Pluton can be distinguished. (i) Xenoliths of metapelitic and metapsammopelitic nature of the contact aureole are seldom observed, except at the northern margin of the Central Rieserferner. Here xenoliths are elongate shaped, with their longest axes parallel to the lineation of the magmatic rocks. Tall xenoliths are a few meters long. Beside their pelitic to psammopelitic composition some of them have a highly deformed mylonitic appearance. Elsewhere in the pluton the xenoliths are restricted to sizes below 20 cm in diameter and are dominated by metapsammopelitic compositions. The magmatic foliation defined by biotite is only slightly deflected around them. (ii) Microgranular enclaves ranging from mafic tonalites to diorites in composition are frequent all over the pluton. In some areas of the Central Rieserferner even swarms of enclaves

were detected with NNW–SSE oriented strikes. The magmatic foliation generally crosscuts the microgranular enclaves, pointing to the low-density contrast of the two melts. Recent investigations on the axial ratios of microgranular enclaves in the Adamello Massive (John and Blundy, 1993; John and Stünitz, 1997) render them good quantitative strain markers. Within the whole pluton oblate shaped enclaves (Fig. 2d) dominate all over, while prolate shapes occur only along the northern margin and may be related to the solid-state overprint.

3.2. Deformation in the country rocks and relationship of syn-intrusive mylonites

The Rieserferner Pluton is surrounded by metapelitic to psammopelitic greenschist facies rocks, with minor occurrences of amphibolites and marbles. Recently the time of fabric development within these rocks has become a matter for discussion. According to the model of Stöckhert (1982, 1985) the penetrative foliation is due to an intense eoalpine isoclinal folding under greenschist facies conditions, while Schönhofer (1999) on the basis of microstructural controlled thermobarometry found evidence for an alpine foliation subparallel to a well preserved variscan foliation. In any case this penetrative foliation predates the late alpine intrusion of the Rieserferner Pluton. The foliation wraps around the pluton with intermediate to steep dips along the southern border and steep to vertical foliations parallel to the contact in the north, that rotate to shallow dips at higher elevations. Isoclinal folds in the roof area are characterised by flat lying axial planes as well. Furthermore observed granitoid apophyses along the eastern margin of the roof show tight to isoclinal folds manifesting the intrusion-related deformation of the country rock.

Along the western border of the pluton, foliations are 30–40° inclined and dip concentrically towards the pluton implying a position of the exposed contact below the plutons equator. This finding is further confirmed by the magmatic and magnetic foliations measured in this area (see below). Within a few tens of meters from the border the country rock foliation strike is rotated parallel to the contact simultaneously with the pre-intrusive fold structures resulting in strongly inclined fold axes.

The northern contact is bordered in large parts by highly deformed mylonitic rocks, for whose continuation to the north of the Eastern Rieserferner no evidence could be found. Clasts within these mylonites denote a sinistral sense of shear. To the north of the central part of the Rieserferner Pluton a range of contact relationships between the intrusive rocks and the mylonites are observed. Numerous granodiorite injections are predominantly found within the mylonites. The injections are boudinaged and strongly lineated parallel to the horizontal or slightly W-plunging mylonitic lineation. The deformation of these granodioritic boudins is less intense than that of the mylonitic host (Fig. 2e). However some of the granodiorites exhibit a gneissic appearance in the field. Less common are fairly undeformed granodioritic apophyses discordantly crosscutting the mylonitic foliation. Hence the mylonitisation is constrained towards the beginning of intrusion, but it ceased before the final emplacement of the pluton. Microstructures indicate an oriented growth of contact metamorphic biotite and sillimanite, confirming the syn-intrusive character of the mylonites. Furthermore, deformation of the mylonites during the final emplacement is suggested by the correspondence of the mylonitic foliation with the variably inclined contact.

Frequently noticed WNW–ESE trending lineations are usually related to the pre-intrusive alpine (?) deformation. However, along the outer contact of the central part of the Rieserferner Pluton the sporadic occurrence of dip lineations within the gneissic non-mylonitic rocks is detected. Contact metamorphic biotite and sillimanite rotated towards the foliation plane (Fig. 2f) point here also to their syn-intrusive growth. This suggests the thinning of the metasedimentary roof of the Rieserferner Pluton. Chessboard patterns in quartz support a high temperature deformation at the contact. On the other hand equilibrated quartz grain boundaries imply a static recrystallisation when temperature was lowered.

4. Microstructures

The accurate genetic interpretation of magnetic fabrics requires detailed study of the microstructures in order to evaluate if rock fabrics are related to magmatic or solid-state deformation. For this purpose thin sections normal to the magnetic fabric axis from about 25% of the sampling sites were cut (see below).

Microstructures within the Rieserferner Pluton are observed ranging between true magmatic deformation and features attributed to a low temperature solid-state deformation. A weak overprint of the magmatic to submagmatic structures is frequently noticed. As long as this overprint is non-penetrative these samples reflect a fabric of magmatic origin. The Central Rieserferner is represented by such samples with the exception of a border along the northern margin adjacent to the mylonites in the country rock. A tendency to a higher amount of solid-state deformation towards the north is distinct at least by the microstructure of quartz and biotite. Within some hundred meters from the northern border the solid-state deformation becomes penetrative. In the field this is indicated by a linear fabric defined by sheared biotite-clusters. In the Western Rieserferner an overprint of the magmatic to submagmatic fabric by solid-state deformation is negligible within the studied samples. Indications for a ductile low temperature solid-state deformation are generally of minor magnitude. To the east along the DAV-Line a late-stage brittle fracturing including the development of micro cataclastic fractures abundantly overprints magmatic structures. This correlates

well with the numerous brittle fractures known from field studies in this area.

4.1. Magmatic to sub-magmatic deformation

Plagioclase is generally lath-shaped with euhedral grain boundaries. The laths own an elongation parallel to the crystallographic *a*-axis and a (010)-plane indicated by the orientation of albite twin lamellae. Together with fairly undeformed biotite-piles they define a weak shape preferred orientation (SPO) in places (Fig. 3a). Non-coaxial magmatic deformation is attested to by imbrication of biotite (Fig. 3b) and plagioclase (Paterson et al., 1998), which is accompanied by the moulding of grain boundaries. A common attribute are intracrystalline fractures in plagioclase with infills of residual melt recrystallised to quartz and minor K-feldspar (Fig. 3c), a characteristic of the submagmatic state of Bouchez et al. (1992). Where plagioclase fills these fractures, twinning planes of the host mineral crosscut the 'veinlet'. Also allanite is affected by submagmatic fracturing. It is normally up to 2 mm long and shows commonly a decomposition rim by epidote and/or clinozoisite. Along the fractures this rim continues, while the centre is filled by quartz.

Quartz and K-feldspar occur as anhedral interstitials in the framework of plagioclase laths and biotites indicating the residual melt (Fig. 3a). K-feldspar lacks any intracrystalline deformation while quartz generally shows besides a weak undulose extinction a typical chessboard pattern (Fig. 3d). The so-called chessboard-patterns are caused by simultaneous prism <a>-and prism <c>-slip of quartz. Temperatures for the latter are constrained to at least 600–700°C (Mainprice et al., 1986, Kruhl, 1996). According to Paterson et al. (1998) the development of chessboards marks the transition between submagmatic deformation and solid-state deformation. Grain boundaries of quartz are strongly lobate due to a high amount of grain-boundary migration recrystallisation (GBMR). The observations of grain-boundary migration at any melt fraction from experiments with non-silicate melts (Means and Park, 1994) have shown that GBMR at least requires a monophase interface.

4.2. High temperature solid-state deformation

Microstructures corresponding to a strain imprint during high temperature solid-state deformation are prominently visible in quartz and biotite. Relicts of chessboard patterns are retained in the centre of rigid quartz grains, while towards the rim these are extinguished by prism <a>-slip acting at lower temperatures. Highly lobate grain boundaries point to GBMR as the active recrystallisation mechanism in quartz. Resulting flattened grains evolve continuously into recrystallised quartz-ribbons, which show generally a rim of fine subgrains.

The homogeneity in the biotite grain size decreases with an increasing imprint of solid-state deformation. Kinks without retrogression to chlorite in the less deformed samples point to the stability of biotite during deformation (Gleizes et al., 1998). Saw-tooth like growth interfaces indicate the recrystallisation of biotite. Amphibole is generally eu- to subhedral with grain sizes up to 5 mm. (100)-growth twins are common (Biermann, 1981). Frequently a retrograde substitution by biotite is observed. In parts sharp grain boundaries between both minerals testify to a high temperature during equilibration. With decreasing temperature basal slip of biotite becomes important and together with the recrystallised quartzes a continuous intercrystalline weak layer (IWL) starts to develop disconnecting the magmatic plagioclase framework (Fig. 3e).

Feldspars are not recrystallised and exhibit only vague undulose extinction within the strongly deformed samples. Nevertheless bent twin lamellae in plagioclase attest some intracrystalline deformation. Myrmekite growth around corroded K-feldspars point to a temperature of around 550°C (Tribe and D'Lemos, 1996). Further crosshatched twin lamellae in K-feldspar suggests the microcline structure.

4.3. Low temperature solid-state deformation

With further decrease in temperature *S–C* fabrics develop. The biotite involved is commonly retrograded to chlorite. The developments of shear indicators like biotite-fishes or oblique quartz-foliations define a predominant sinistral sense of shear (Fig. 3f). Quartzes are characterised by highly undulose extinction and subgrain boundaries. Grain boundaries show remarkable 'bulges', indicating grain boundary migration at low temperature (Hirth and Tullis, 1992). Brittle deformation of quartz is further attested by fracturing.

Lately Paterson et al. (1998) suggested a secondary alteration of the magmatic minerals to be coupled with low temperature solid-state deformation. However, intrusive rocks of the Rieserferner Pluton frequently show bands of light green material corresponding to the substitution of biotite by chlorite. Since deformation is no stronger within these bands (epitaxial chlorite replaces biotite) a large part of retrograde metamorphism must be related to a late-stage migration of hydrothermal fluids. Therefore care is taken not to over-emphasise this feature as pointing to a high amount of solid-state deformation.

5. Anisotropy of magnetic susceptibility

5.1. Methods

The application of AMS techniques on detailed structural mapping of granitic rocks has now been used for almost four decades since the work of Balsey and Buddington (1960) and Stacey (1960). Henry (1975) applied the method on the Rieserferner Pluton and its country rock. Nowadays AMS is routinely used for structural investigation on granitoids that appear massive in the field (Hrouda and Lanza, 1989;

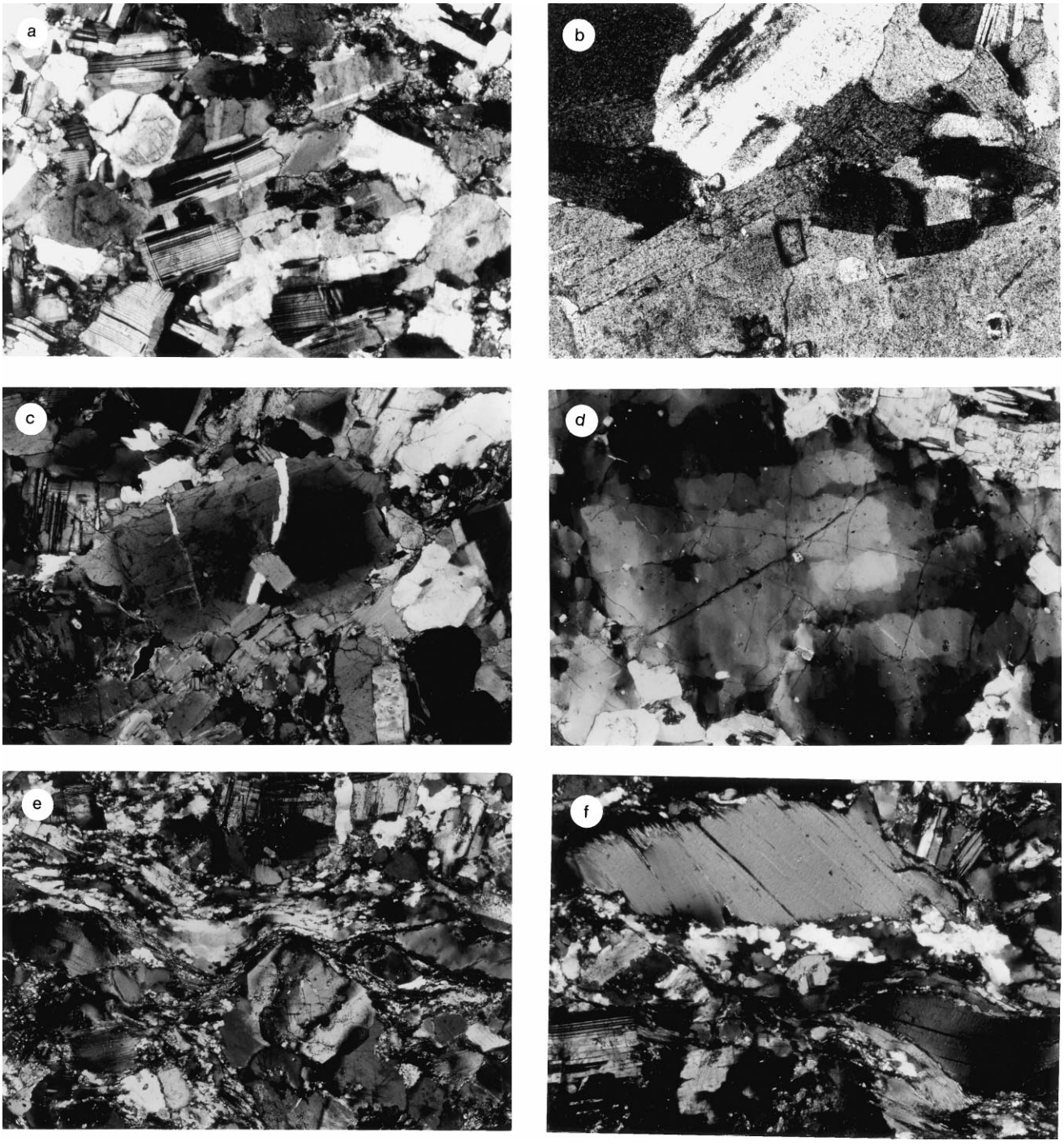

Fig. 3. (a) A magmatic foliation (left to right) is shown by a linear arrangement of tabular plagioclase crystals. Lamellae of albite growth twins are parallel to the foliation (width of view 3 mm, CPL). (b) Tiling of biotite points to non-coaxial magmatic flow fabric (width of view 15 mm, CPL). (c) Fractures in plagioclase are filled with quartz and K-feldspar, indicating the submagmatic stage (width of view 1.2 mm, CPL). (d) Chessboard patterns in quartz-core attest the transition between the submagmatic stage and the field of high temperature solid-state deformation. Recrystallisation of quartz within this stage of deformation is not observed (width of view 2.3 mm, CPL). (e) Elongate quartz crystals and ribbons of recrystallised quartz indicate the decrease in temperature during deformation. Biotite and quartz develop a continuous intracrystalline weak layer (IWL), disconnecting the former plagioclase framework (width of view 10 mm, CPL). (f) Biotite fishes record sinistral sense of shear, which confirms the regional sinistral transpressive deformation along the DAV-Line and the mylonites to the north of the Rieserferner Pluton (W is to the left) (width of view 1.2 mm, CPL).

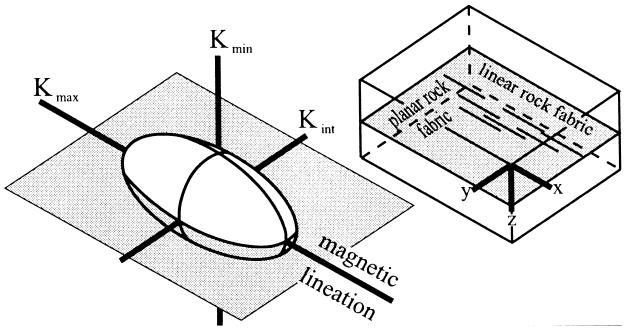

Fig. 4. Relationship between the magnetic fabric ellipsoid and the macroscopic fabric of the intrusive rocks of the Rieserferner Pluton. K_{max} parallels the macroscopic lineation (x-direction) related to magmatic flow or solid-state deformation, while K_{min} is normal to the foliation (x–y-plane) generally defined by the arrangement of tabular shaped crystals like biotite and plagioclase.

Bouchez et al., 1990; Gleizes et al., 1998). A wealth of papers has been published discussing the relationship between rock fabrics and magnetic fabrics (e.g. Hrouda, 1982; Siegesmund et al., 1995; Bouchez, 1997) the essence being that AMS provides a fast determination of foliations and lineations, the latter being hard to observe in the field. The theoretical background of the AMS measurement is described elsewhere (e.g. Hrouda, 1982, Rochette, 1987, Rochette et al., 1992). For most geological materials magnetic susceptibility is an anisotropic property which can be described mathematically by a second rank tensor or geometrically represented by a triaxial magnetic fabric ellipsoid with the three half axes $K_{max} > K_{int} > K_{min}$, whose mean value is the bulk susceptibility magnitude. The AMS of a rock sample is controlled by the paramagnetic and ferrimagnetic (s.l.) behaviour of the rock forming minerals. The influence by diamagnetic minerals is negligible. For granitoids the iron bearing silicates, especially biotite and amphibole, carry paramagnetic properties. In this case the magnetic fabric ellipsoid can be directly related to the crystallographic preferred orientation (CPO) of the paramagnetic carriers (Fig. 4). In ferrimagnetic granites paramagnetic properties may be obliterated by the high intrinsic susceptibility of iron bearing ore minerals, like hematite and magnetite. Magnetic fabrics in such rocks should be related to a primary shape anisotropy of magnetite grains or may also result from an inhomogeneous grain distribution (for a review see Rochette et al., 1992). To check the ferrimagnetic contribution on the magnetic properties of the investigated granitoids representative samples were measured in higher magnetic fields (HFA) ranging from 0.8 to 1.8 T using a torque magnetometer (Bergmüller and Heller, 1996). Moreover, curie balance measurements were realised for a quantitative analysis of ferrimagnetic carriers at an applied magnetic field of 0.55 T and a maximum temperature of 700°C.

In order to obtain a full magnetic fabric pattern over the whole pluton nearly 170 handspecimens were collected, corresponding to a sample density of at least two sampling sites per square kilometre (Fig. 5a). Sample orientation was done via compass measurement on marked plane surfaces.

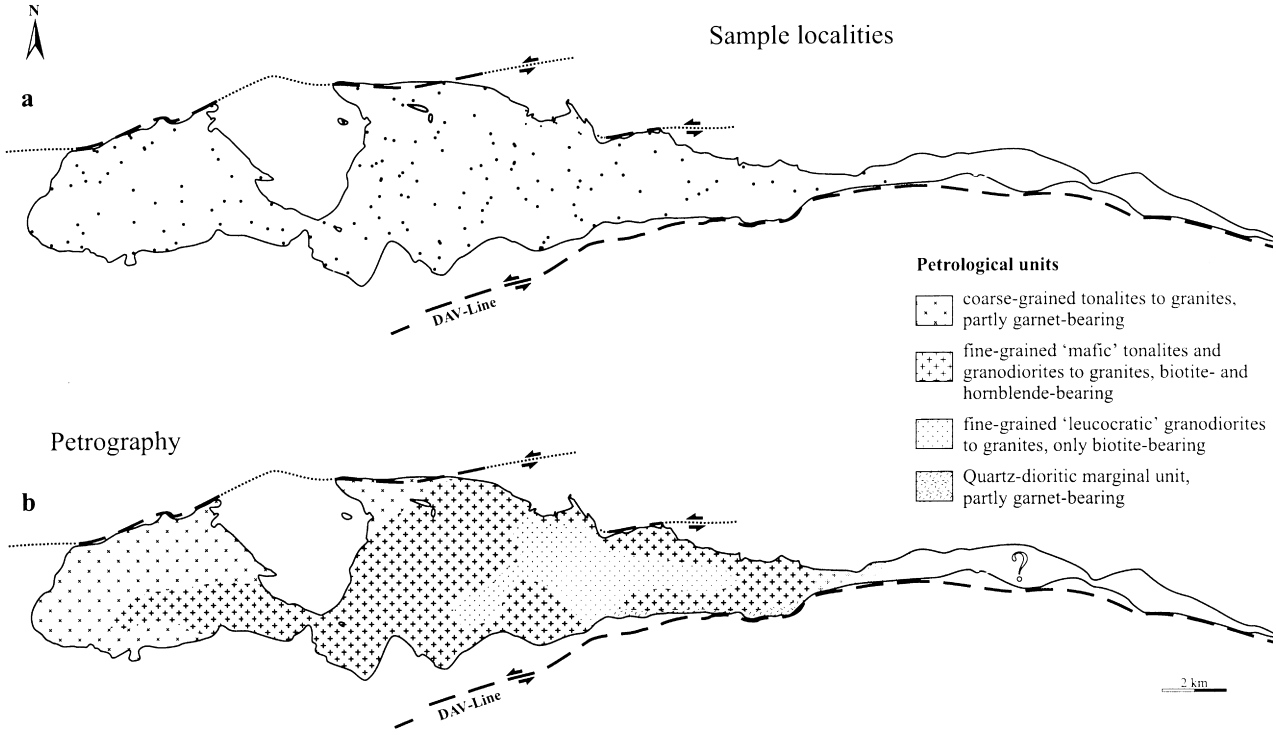

Fig. 5. Sketch map of the Rieserferner Pluton. (a) Black dots indicate sample localities. (b) differently shaded zones refer to the petrological zoning inferred from field observation, geochemical data and bulk susceptibility measurement. Note the sinistral DAV-Line partly bordering the Rieserferner Pluton in the south and the mylonites to the north of the pluton intersecting the contact of the Central Rieserferner.

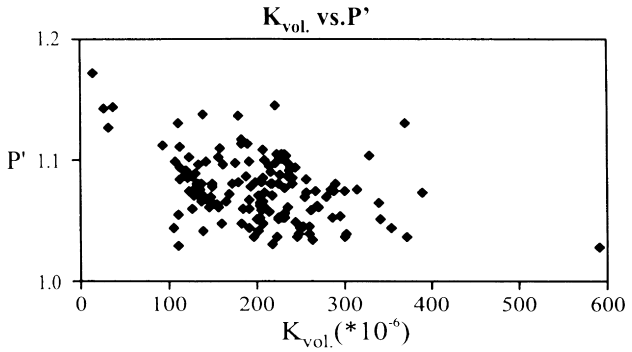

Fig. 6. Degree of anisotropy (P') versus bulk susceptibility (K_{vol}) for the intrusive rocks of the Rieserferner Pluton from all sample sites. Low values for P' of <1.2 and K_{vol} generally $<400 \times 10^{-6}$ are explained by paramagnetic carriers.

The variation in sample density is due to the lack of outcrops in the area of boulder fields and glaciers and the difficult access in some extremely exposed regions. From each of the specimen a minimum of 2×2 standard-sized cores with a diameter of 25 and 40 mm and a height of about 87% the diameter were drilled and reoriented in a sandbox. The magnetic fabric determination from nine different directions for each core sample was carried out with a Kappabridge KLY-2 (manufactured by Geofyzika, Brno) working at 4×10^{-4} T and 920 Hz, with a detection limit of 4×10^{-8} SI. From this follows the magnetic fabric ellipsoid, which is computed using the 'ani20' program of Jelinek (1977). From each sample site one core sample was selected representing the approximate mean of the measurements. The coherence between individual core samples from one sample site is generally good. Only some coarse-grained samples show a wide variation of magnetic parameters. Nevertheless, bigger cores generally exhibit even in those samples a low scatter in magnetic properties and directional data. So in these cases the bigger cores are taken to be representative for a sample site. For presentation of the magnetic fabric data P' and T proposed by Jelinek (1981) were chosen. P' is the degree of anisotropy of the magnetic fabric ellipsoid taking into account the intermediate semi-axis of the ellipsoid, while T is the shape factor of the AMS ellipsoid, ranging from −1 to 0 to + 1 referring to a prolate, neutral and oblate shape, respectively.

5.2. Bulk susceptibility versus petrography

Values for bulk susceptibility from the investigated core samples generally range from 30×10^{-6} to 400×10^{-6} SI. Low bulk susceptibility down to 6×10^{-6} SI is restricted to late-stage aplitic dykes. The high bulk susceptibility of nearly 600×10^{-6} SI measured in one sample next to the contact indicates the presence of ore minerals here (Fig. 6). Taking P' into account which is generally <1.2, bulk susceptibility values point to a control of the magnetic fabric by paramagnetic minerals (Rochette, 1987).

A broad variation in the bulk susceptibility of several

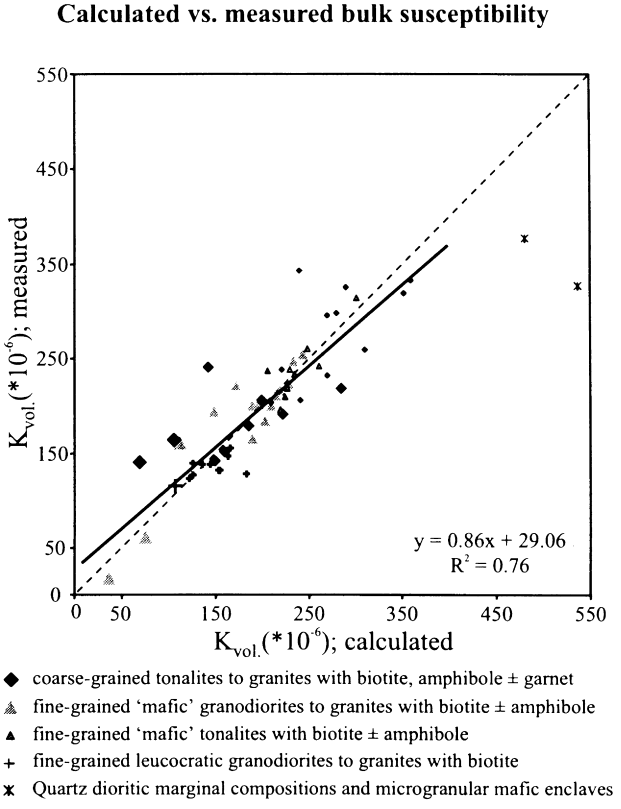

Fig. 7. Comparison of the measured versus a calculated bulk susceptibility value based on the Fe^{2+}, Fe^{3+} and Mn^{2+} content (Gleizes et al., 1993). The ratio for a large part of compared samples is ~1. The different magmatic subunits are well defined by their ranges in bulk susceptibility, with the exception of the coarse-grained granitoids of the Western Rieserferner, spreading off over the observed range. Differently sized symbols suggest the magmatic fractionation from tonalite (small symbols) to granite (tall symbols).

orders in magnitude is reported for many magnetite-bearing granites (e.g. Saint Blanquat and Tikoff, 1997; Siegesmund and Becker, 2000). Within such intrusives susceptibility measurements reflect the petrological zoning of the complex and provide a good petrological mapping tool. In case of low bulk susceptibility plutons the demonstration of a petrological zoning should be based on geochemical investigation. But even in those plutons the bulk susceptibility could reflect the different fractionated magma batches fairly well (Gleizes et al., 1993, 1998). Bellieni (1978) and Bellieni et al. (1981) demonstrated a complex magmatic history of the Rieserferner Pluton. In the present study it was observed that strong fractionation of the magma is documented by a broad scatter of bulk susceptibility values taking the total petrological variability into account (Fig. 5b). However, looking at each individual magma subunit a tight correlation between the measured bulk susceptibility and a calculated susceptibility based on the geochemical data of Bellieni (1978), is reflecting the magmatic differentiation within each batch (Fig. 7). For calculation of the bulk susceptibility using geochemical data the formula by Rochette et al. (1992) in its modified version (Gleizes et al., 1993) was

applied taking into account the Fe^{2+}, Fe^{3+} and Mn^{2+} contents as well as the specific paramagnetic Curie temperature. The following average ranges of measured magnetic susceptibilities correlate with petrological zoning: $K_{vol} < 10 \times 10^{-6}$ SI = aplites and pegmatites; 110×10^{-6} SI $K_{vol} < 160 \times 10^{-6}$ SI = fine-grained leucocratic granodiorites to granites with biotite; 130×10^{-6} SI $< K_{vol} < 320 \times 10^{-6}$ SI = fine-grained 'mafic' tonalites and granodiorites to granites with biotite ± amphibole; 130×10^{-6} SI $< K_{vol} < 600 \times 10^{-6}$ SI = coarse-grained tonalites to granites with biotite, amphibole ± garnet; $K_{vol} > 300 \times 10^{-6}$ SI = Quartzdioritic marginal compositions and microgranular mafic enclaves.

The coarse-grained granitoids of the western periphery show a wide scatter of bulk susceptibilities covering almost the whole observed range (Fig. 7). A differentiation is possible only taking into account their appearance in the field. The other lithological types of the Rieserferner Pluton show reduced average ranges in bulk susceptibilities. Though being conspicuous in the field a gradual transition between the coarse-grained granitoids and the 'mafic' granodiorites is not detected via bulk susceptibility measurement.

5.3. Significance of magnetic fabrics

To confirm the magnetic data U-stage measurements on (001) biotite basal planes were carried out. A good correlation between the shape of the AMS ellipsoid and the biotite (001) normal distribution is apparent. Prolate AMS fabric ellipsoids correspond to weak to almost perfect girdle patterns of the basal planes, while point maxima are consistent with an oblate AMS fabric ellipsoid (Fig. 8). Small differences between AMS orientation and the biotite (001) textures are attributed to differences in volume sampled by the two methods.

The AMS data was improved by the HFA technique in order to exclude a significant ferrimagnetic contribution to the magnetic fabric. The combination of HFA and AMS allows the separation of paramagnetic and ferrimagnetic properties (Siegesmund and Becker, 2000). For comparison between AMS and HFA data U is used instead of the T parameter, because the torque magnetometer measures the deviatoric part of the magnetic fabric tensor only. Two samples R2 and R96 are presented with a shape factor of $T = -0.34$ ($U = -0.35$) and $T = 0.62$ ($U = 0.61$), respectively. U parameter and directional data from HFA measurement are in good accordance with the AMS data (Fig. 9a). A weak scatter of K_{int} and K_{max} along a great circle for sample R96 is in agreement with an oblate magnetic fabric ellipsoid. Moreover, curie balance measurements could not be interpreted in terms of any significant contribution of ore minerals within the samples (Fig. 9b).

Besides the orientation data, the magnetic susceptibility provides qualitative information about magnetic fabric geometry usually expressed as P' and T (Jelinek, 1981) referring to the degree of anisotropy and the shape of the magnetic fabric ellipsoid respectively. A graphical correlation for the Rieserferner Pluton of P' versus T shows a wide range of P' for oblate AMS fabrics while prolate fabrics correspond predominantly to low degrees of anisotropy (Fig. 10). Dominantly magmatic to submagmatic microstructures correspond to oblate magnetic fabrics. Therefore magnetic fabrics are regarded to present indirectly the geometry of strain during magma chamber processes. Since the magmatic deformation memory reflected by the AMS data is rather short (Bouchez, 1997), care should be taken with an over-interpretation of these data.

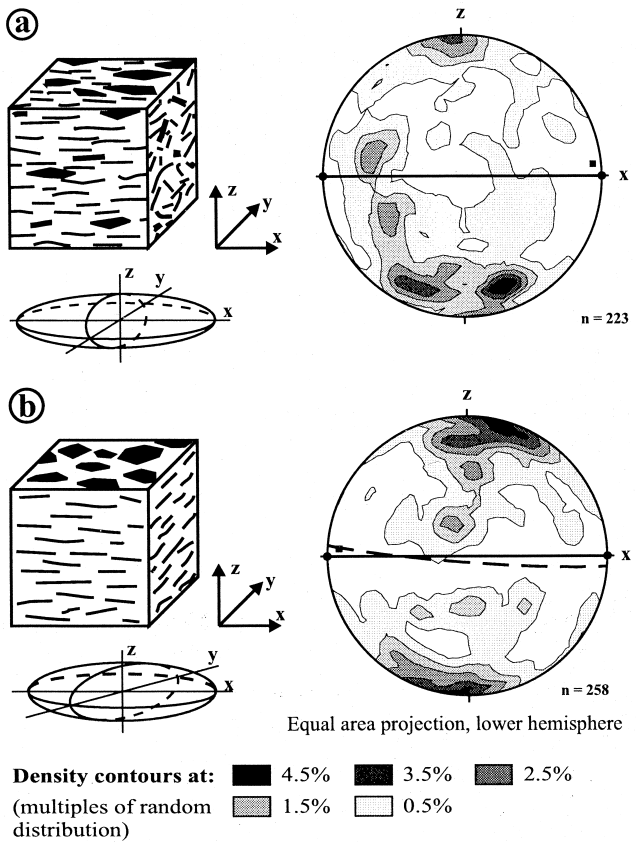

Fig. 8. Comparison between macroscopic fabric, shape of the magnetic fabric ellipsoid and biotite (001) pole distribution. Observed magnetic fabrics of the two granitoids represent a wide range from prolate to oblate shaped magnetic fabric ellipsoids. The two samples typically represent the solid-state deformed northern margin of the Central Rieserferner (a) and the magmatic to submagmatic microstructures of the Central Rieserferner close to the western contact and the roof (b). (a) The cube represents schematically the rotational arrangement of tabular biotite crystals, causing the prolate shape of the magnetic fabric ellipsoid (line drawing). Biotite (001) poles form a near perfect girdle. (b) Planar arrangement of biotite crystals results in an oblate shaped magnetic fabric ellipsoid (line drawing) which corresponds to a pronounced biotite (001) pole distribution maximum. Pole figures are standard projections with magnetic foliation (x–y-plane) and K_{max} (x-direction) horizontal (solid line and black dot). The filled black squares marks the macroscopically observed lineation, while the dashed line (only in b) represents the macroscopic foliation which is in good agreement with the AMS data.

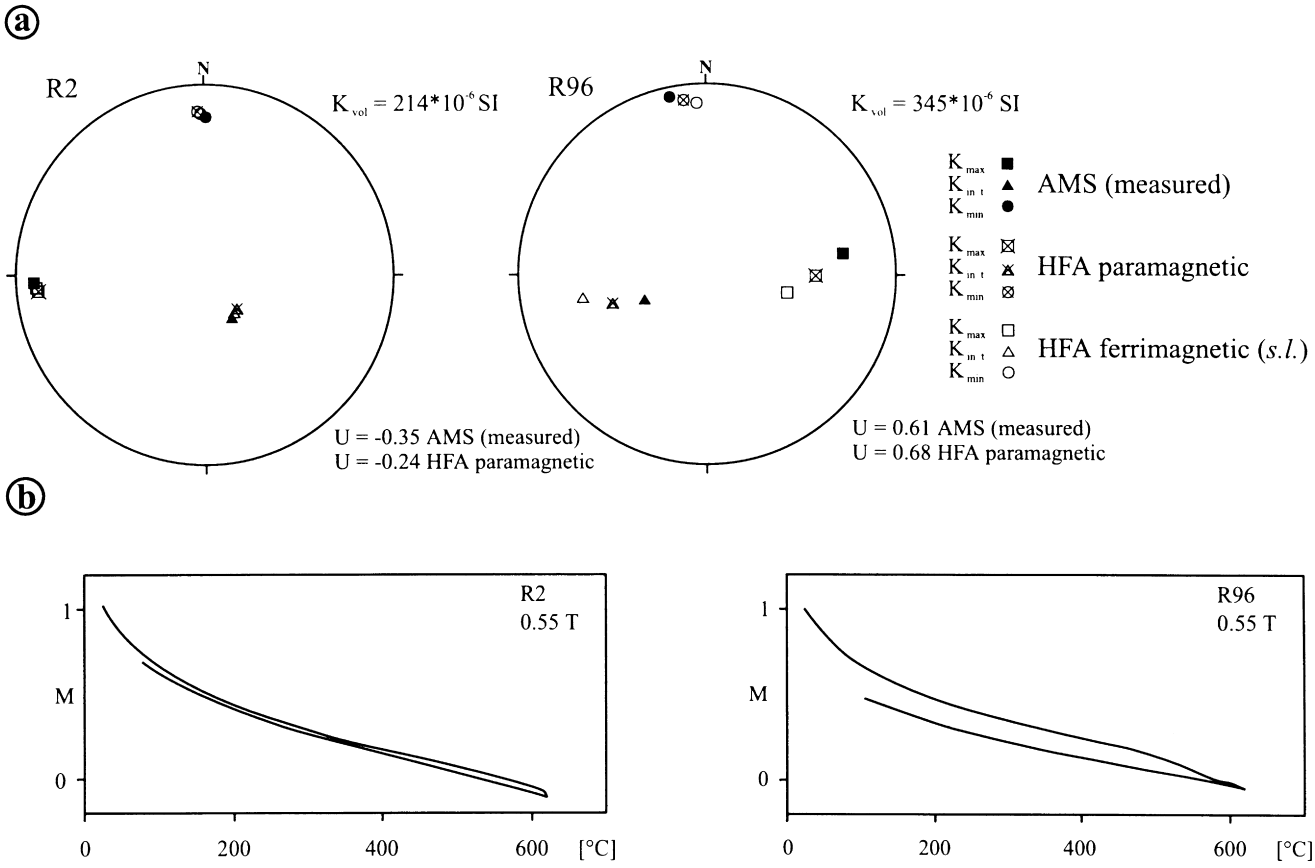

Fig. 9. (a) Comparison of the magnetic axes from separated paramagnetic and ferrimagnetic contributions and the measured AMS fabric from a characteristically prolate (R2) and oblate (R96) magnetic fabric sample. Further the U-parameter obtained from AMS measurement and the paramagnetic contribution of the HFA is given. Note also the bulk susceptibility value which is below empirical data of typical magnetite bearing granitoids. (b) Thermomagnetic curves from the two samples above displaying magnetisation M in a field of 0.55 T vs. temperature (°C) measured in vacuum and at a heating rate of 20°/min. The curves can not be explained in terms of any significant ferrimagnetic contribution to the magnetic properties.

Rochette et al. (1992) put emphasis on the problem of mixed fabrics owing to at least two paramagnetic minerals. Since single crystal data of these minerals, commonly biotite and amphibole in a magmatic intrusive exhibit a different magnetic fabric ellipsoid the variation of magnetic parameters is likely to be mainly due to the compositional variation, rather than to increasing strain. Numerical models (Siegesmund and Becker, 2000) confirm this. They found magnetic parameters highly affected, if both phases are textured, while the influence of an isotropic distribution of one paramagnetic carrier will not shift the values significantly. In case of the Rieserferner Pluton the magnetic fabric is carried mainly by biotite. An possible influence by high modal contents of amphibole on the magnetic fabric is restricted to the Western Rieserferner.

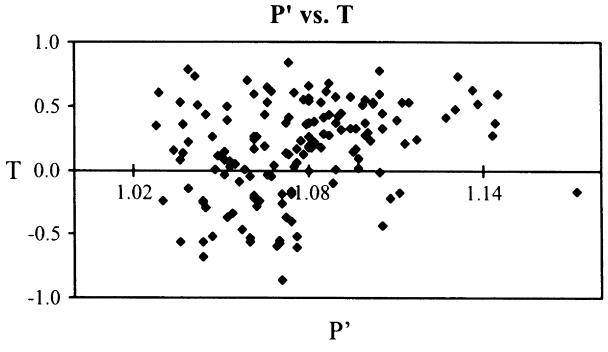

Fig. 10. Variation of T versus P'. The shape parameter T of the magnetic fabric ellipsoid covers nearly the whole range from perfect oblate to prolate fabric, respectively from +1 to −1. The degree of anisotropy (P') is restricted to a small array from 1.04 to 1.17. Furthermore, this range is reduced to values generally <1.12 for prolate magnetic fabrics. It is inferred that flattening is the strain regime prevailing in the emplacement fabrics.

5.4. Directional data

Directional data provided from the AMS was carefully compared with the macroscopic foliation observed prior to the magnetic measurement. This control is mainly restricted to the planar fabric due to the lack of exposed foliation surfaces that show any linear arrangement of minerals. Nevertheless, in some places also a linear fabric is noticed, which was found to parallel K_{max}.

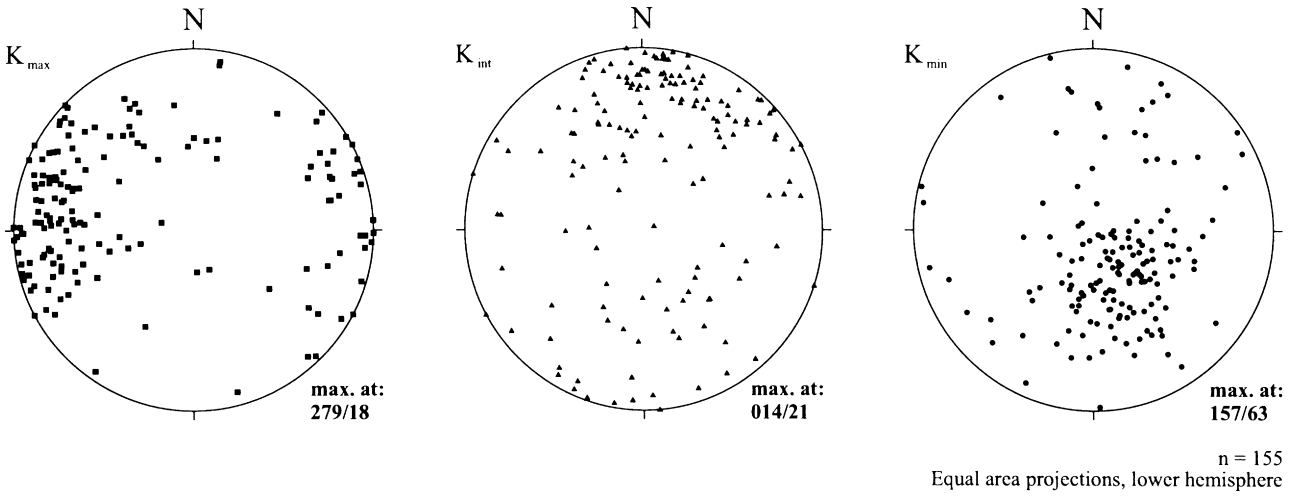

Fig. 11. Pole distribution of the magnetic fabric axes of the Rieserferner Pluton (equal area projection, lower hemisphere): K_{max} is the magnetic lineation and K_{min} normals the magnetic foliation plane (K_{max}–K_{int}-plane). The magnetic lineation shows a general westward plunge, while the foliation normal exhibits a strong point maximum at 157/63 and a weak scatter along a great circle (110/70) normal to the lineation mean.

The axes of the magnetic susceptibility ellipsoid are well defined considering the deviations between cores for individual sample sites. Scattered distributions for K_{int} and K_{min} along great circles in a stereographic projection arise particularly within a few samples from the northern margin of the pluton. This is in good agreement with the linear macroscopic fabric and the prolate shaped microgranular enclaves of those rocks. K_{max} is commonly well defined. However, some locations exhibit a scatter in the K_{max} direction comparing the individual core samples. Those sites generally exhibit highly oblate magnetic parameters ($T > 0.7$) and low lineation factors ($K_{max}/K_{min} < 1.006$). This points to a minor significance of their lineations. K_{min} directions exhibit a weak girdle distribution, while the magnetic lineation (K_{max}) plunge predominantly to the west with a mean normal to the great circle defined by K_{min} (Fig. 11). This is in accordance with the previous AMS study of the pluton (Henry, 1975).

The foliations of the Rieserferner Pluton describe at least three different interconnected dome structures that are related to the three parts of the pluton (Fig. 12a). Within the Central Rieserferner the foliation trajectories form an asymmetric dome structure with intermediate to steep south-dipping foliations next to the DAV-Line and at the border to the Western Rieserferner, while to the north slightly outward dipping foliations were observed that become progressively steeper towards the contact. Foliations parallel the contact to the south and west, while in the north they are oblique to the contact, but still parallel to the mylonitic foliation in the country rock. The centre of the dome structure as suggested by the arrangement of the foliation trajectories is located to the south–east close to the plutons margin.

In the Western Rieserferner the foliation trajectories parallel the contact where exposed. The dip of the foliation is variable but shows a weak tendency for an inclination outward from the core axis, which is located in the south of the Western Rieserferner. The high variability of the foliation dip is caused by a predominance of L-fabrics. At the western margin of the pluton foliations are slightly inward dipping and trace the contact. Therefore the exposed contact is expected to be in a position somewhere below the equatorial plane of the intrusive.

At least one more ellipsoidal complex could be reconstructed within the eastern part of the Rieserferner Pluton. In this area the plutons southern border is directly marked by the DAV-Line. Here the foliations are changing from dipping north to dipping south within a narrow zone along the DAV-Line. Further to the east limited structural observations are hard to interpret. At least a foliation strike parallel to the outline of the Pluton is noticed.

Within the Central Rieserferner the lineation exhibits a wide curved pattern with WNW plunging lineations in the east and southeast and E–W trending lineations to the west (Fig. 12b). This lineation bow is sigmoidally deflected along the northern contact as well as to the south, where the DAV-Line is close to the contact, reflecting the syn-intrusive regional sinistral movements. The plunge is predominantly towards the west (mean at 279/18) increasing toward the south-western part of the Central Rieserferner. The E–W trending and further to the north ENE–WSW trending lineation of the Western Rieserferner is highly variable in inclination. Also, in this part of the pluton some NW–SE trending lineations are observed. Steep lineations at the transition between the Central and Western Rieserferner do not fit the general lineation pattern but plunge with right angles to the general strike. For the Eastern Rieserferner predominantly N to NW plunging moderately to steeply dipping lineations were obtained.

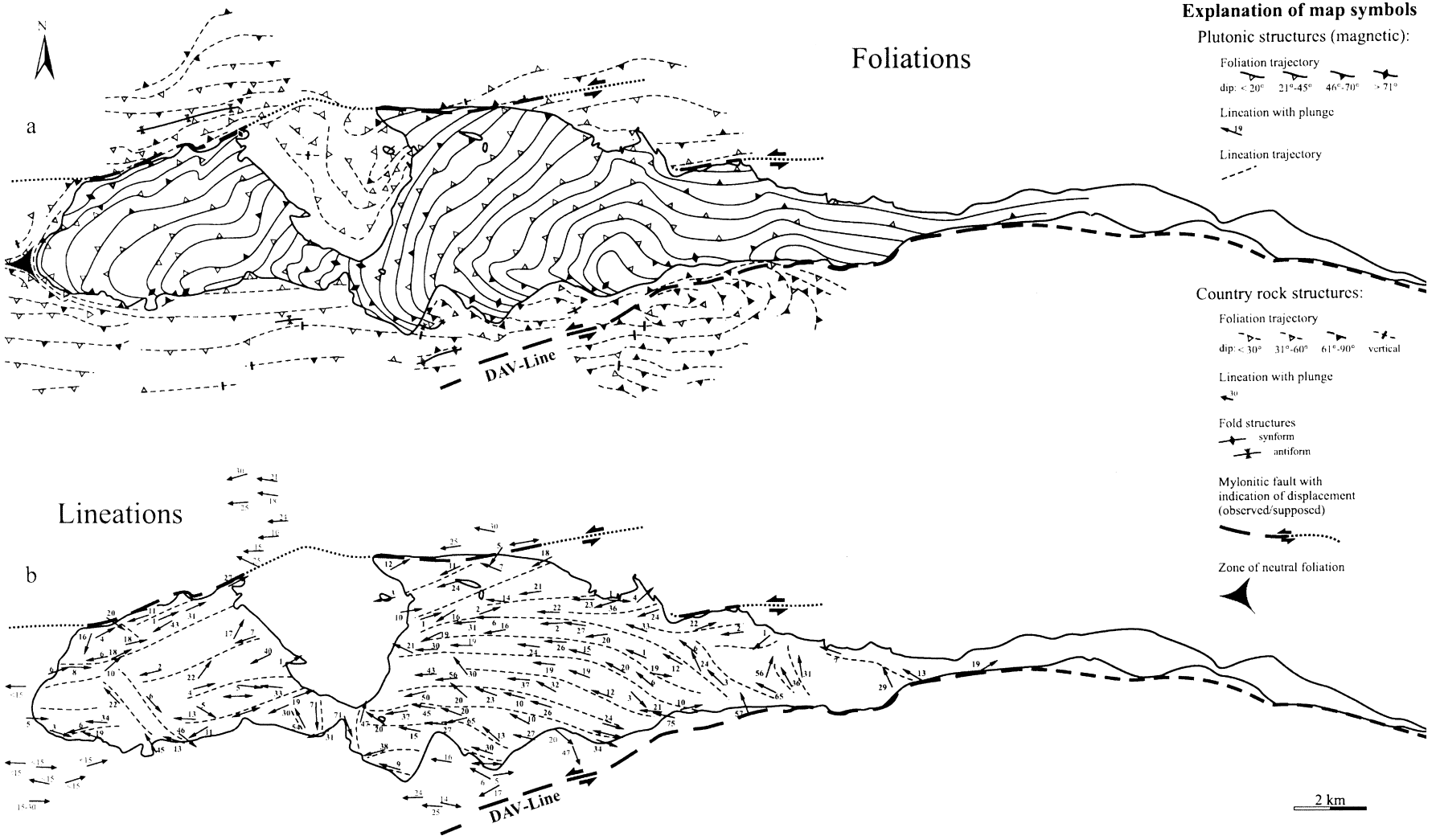

Fig. 12. Directional data of the Rieserferner Pluton. (a) Foliation trajectory map of the pluton. The foliation crosscuts internal contacts of the different magmatic subunits. In the Central Rieserferner the foliation is parallel to the southern and western contact, while to the north the contact is intersected by the foliation. (b) Lineation map of the pluton. The magnetic lineation is predominantly E–W oriented. Exceptional is the northern border of the Central Rieserferner, where the lineation trend is ENE–WSW. Further to the east the lineation is weakly sigmoidal deflected at the southern contact. The sporadic occurrence of NW–SE trending lineations in the Western Rieserferner may point to a late alpine E–W compression of the massif under solid-state conditions (Henry, 1975).

6. Implications for the emplacement of the Rieserferner Pluton

Foliation and lineation appear not to be co-magmatic since they crosscut magmatic banding and even some late-magmatic dykes. On the other hand there are large domains with dominantly magmatic microstructures and the foliation pattern forms domes suggestive of magmatic controls. In the following section we will try to reconcile these seemingly contradictory observations. Also, we will explore the role taken by the DAV-Line's sinistral strike slip regime during the emplacement and the deformation of the pluton.

Contact relationships and geochemical data (Bellieni et al., 1978; Bellieni et al., 1981; Schönhofer, 1999) indicate that the amphibole-rich, garnet-bearing tonalitic to granodioritic peripheral types from the west and north–west are the early magmas of the Rieserferner Pluton. They are followed by the fine-grained tonalitic and granodioritic to granitic batches further to the east (Fig. 5). Insufficient exposure of the pluton in its eastern part restricts the relative timing of the intrusion to geochemical arguments. Highly evolved leucocratic granodioritic to granitic compositions (Schönhofer, 1999) are assumed to indicate the last magmatic event during the emplacement of the Rieserferner Pluton. They were preceded by garnet-bearing quartz-diorites locally outcropping along the southern margins of the Eastern Rieserferner (Fig. 5). So the petrologic/geochemical findings point to an overall west to east intrusion sequence of several increasingly differentiated magma batches.

Evidence for a particular emplacement mechanism must be carefully evaluated. A large amount of stoping (Daly, 1933) controlling ascent of magma can be excluded on the strength of the rare occurrence of metasedimentary xenoliths throughout most of the pluton. Only in the north of the Central Rieserferner several deka-meter scale xenoliths are observed within the coarse-grained rocks making it conceivable that in the beginning emplacement was accompanied by stoping.

Recently Mager (1985) suggested a lateral dislocation gradient to one side of the DAV-Line so that the ensuing dilatation provided space for the ascending magmas of the Rieserferner and Zinsnock. He used the 'remarkable knee' of the band of orthogneisses to the north of the Rieserferner Pluton (Fig. 13) to support his hypothesis. Recent structural investigations on the Sand in Taufers orthogneiss show however that its outcrop pattern is the effect of pre-intrusive fold structures rather than kilometre scale steep folding during the emplacement of the Rieserferner Pluton (Mazzoli, oral communication) caused by an inferred dislocation gradient. Different geochemical composition of the Zinsnock and Rieserferner make a subsurface connection of the plutons highly speculative. Similar geochemical compositions of the Zinsnock Pluton and the evolved magmas of the Eastern Rieserferner (Schönhofer, 1999) may indicate a relationship late in the emplacement history which so far is poorly understood.

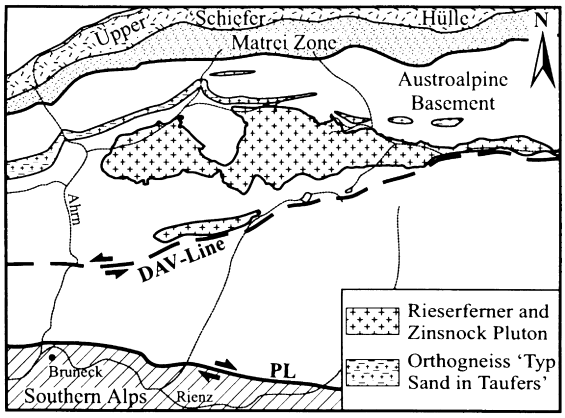

Fig. 13. Simplified sketch map of the Rieserferner and Zinsnock Plutons and the Ordovician 'Sand in Taufers' Orthogneiss. Note the conspicuous 'knee' of the orthogneisses directly to the north of the Rieserferner Pluton. Recent structural observations show that the outcrop pattern of the orthogneisses is related to variscan deformation rather than folding around steep axes caused by a lateral dislocation gradient to the north of the DAV-Line during the emplacement of the Rieserferner Pluton.

Nevertheless, faulting should have had a large influence on ascent and expansion of the magmas as is indicated by the syn-intrusive mylonites along the northern contact. Concentric foliation trajectories with a centre to the south–east in the Central Rieserferner Pluton may suggest the DAV-Line as feeder zone for the ascending magmas. Since fabric elements crosscut internal contacts within the pluton they postdate the juxtaposition of the different subunits, and thus can at best provide only indirect information on the location of magma ascent. This could be the case where foliation formed by way of thermal stresses and differential buoyancy of individual magmatic subunits outlasting the magmatic emplacement. Microstructures tell us that over large parts of the pluton this should have occurred in the submagmatic or high temperature regime prior to final solidification. Magma accommodation is thought to follow the direction in which space is created by the successive widening of a pull apart structure. Pull apart should have resulted from displacement transfer between the DAV-fault in the South to the synintrusive mylonites north of the pluton (Fig. 14).

For the Western Rieserferner it is believed that observed fabrics still largely reflect the magmatic flow during intrusion (Fig. 14). This is strongly suggested by the magmatic to sub-magmatic microstructures, a low degree in magnetic anisotropy (P' is around 1.06) and a high variability of the shape factor. E–W to ENE–WSW trending lineations with a variable plunge support an E–W oriented flow pattern of the magma. The rare occurrence of NW–SE trending lineations may correspond to a post-intrusive compression of the massif (Henry, 1975).

Syn-intrusive folding in the metasedimentary roof next to the contact of the Central Rieserferner as well as textured

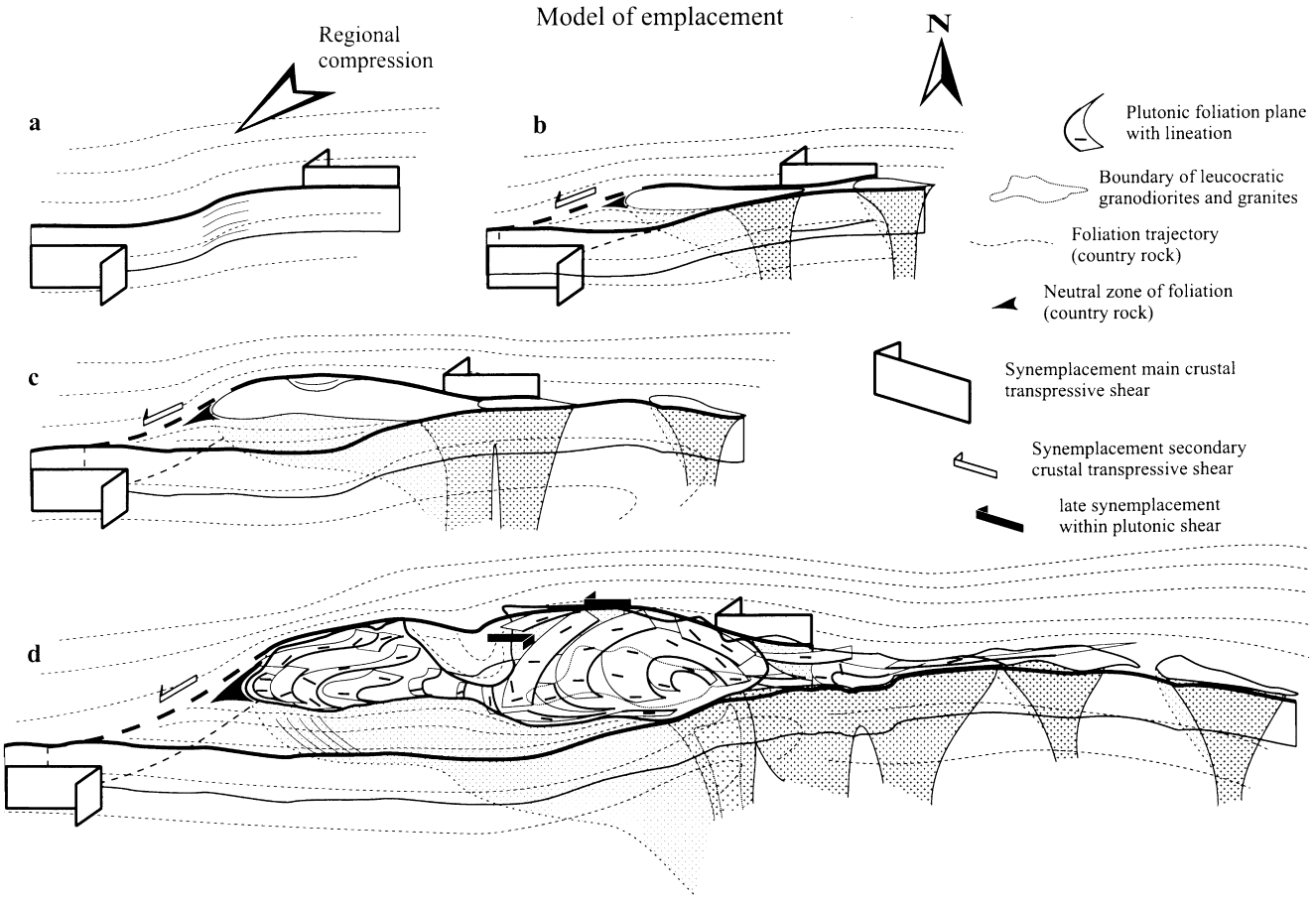

Fig. 14. Model of the emplacement of the Rieserferner Pluton and coeval regional transpressive sinistral deformation. (a) Supposed initial situation. (b) Assumed development of a pull-apart structure that provides space for the ascending magmatic precursors of the Rieserferner Pluton. (c) Progressive magma ascent in the opening pull-apart structure, while individual magma batches further to the east rose up along the DAV-Line. (d) Final position of the Rieserferner Pluton. The Central Rieserferner suffers some ballooning due to the ascent of the last granodioritic magma batch.

growth of contact metamorphic sillimanite record aspects of a more complex intrusion history for the Central Rieserferner. Prominent oblate magnetic fabrics correspond with magmatic to submagmatic microstructures with a strong shape preferred orientation of tabular shaped crystals as a consequence of flattening strain during solidification of the magma. The remarkable increase in the degree of anisotropy ($P' > 1.06$) particularly towards the western border of the Central Rieserferner is regarded to reflect increasing magmatic and/or submagmatic deformation towards the contact. We infer that flattening is the response to a final spherical expansion of the pluton caused by the late intrusion of the leucocratic granodiorites similar to the ballooning of the Flamanville Granite (Brun et al., 1990). The rare occurrence of prolate magnetic fabrics correlates with high-temperature solid-state deformed granitoids. They provide no information on the emplacement but show that the pluton suffered syn- to post-intrusive mylonitisation along its northern contact (Fig. 14). The lack of low-temperature solid-state deformation features within the deformed granitoids attest that mylonitisation ceased shortly after the final emplacement. Recently Rosenberg et al. (1995) proposed for the Bergell Pluton a final emplacement by ballooning along the dextral transpressive Tonale Line (Fig. 1), which corresponds well with our results on the Rieserferner Pluton. Observing syn-intrusive folds near the floor of the pluton they conclude that the Bergell Pluton formed from magma squeezed from the shear zone.

So far our structural information on the Eastern Rieserferner is very limited. Nevertheless, magmatic structures with minor cataclastic overprint may testify to the original shape of the tail of the Rieserferner. Despite an elongate tail being common to the Rieserferner and the Bergell Plutons their origins are entirely different. Rosenberg et al. (1995) could show that the tail of the Bergell represents the feeder for the ascending magmas and the deepest part of the pluton. Following the final emplacement the Bergell Pluton was tilted exposing the feeder. In the case of the Rieserferner Pluton highly fractionated granodiorites and granites of the tail point to a late emplacement. Furthermore, apparent tilting of the crustal block to the north of the DAV-Line indicates the largest uplift in the west (Borsi et al., 1978). So the tail of the Rieserferner represents the shallowest and least exhumed part of the pluton.

7. Conclusions

Magnetic fabrics of the Rieserferner granitoids essentially reflect biotite textures with presumably slight admixtures of hornblende the latter showing little preferred orientation. Where it can be observed macroscopic and microscopic orientation of foliation and lineation are close to the magnetic fabric elements. Deviations can be attributed to differences in sample size combined with the low strength of granitoid fabrics.

The foliation crosscuts primary banding and internal contacts. Yet based on microstructure the observed foliation domes formed largely during the submagmatic stage and prior to solidification. The foliation domes may reflect magma ascent if foliation is caused by stresses due to buoyancy and changes in volume of individual subunits. Though these processes outlasted the magmatic stage a certain inheritance of magmatic preferred mineral orientation is indicated by the microstructures.

A sigmoidal bend of the lineation in the Central Rieserferner conforms with left lateral shear affecting the intrusion during the submagmatic stage. This deformation could partially also have contributed to the shaping of the foliation domes.

Solid-state deformation is pervasive only near the steeply inclined contacts along the bordering mylonitic shear zones. Markedly prolate magnetic fabrics in accordance with macroscopic prolate fabrics occur in the north of the Central Rieserferner reflecting the syn-intrusive sinistral shear.

The locus of intrusion seems to be regionally controlled by the southward bend of the DAV-Line. Space is provided by pull-apart due to displacement transfer between the left-lateral transcurrent DAV in the south to the syn-magmatic mylonites on the northern margin of the intrusions.

Late-stage emplacement processes are local modest ballooning as evidenced by predominance of oblate magnetic fabrics and oblate enclaves near the roof of the Central Rieserferner. Large xenoliths near the northern edge of the Central Rieserferner may point to limited stoping during the early stages of intrusion.

Acknowledgements

Constructive information and unreserved discussion in the office and during field excursions with B. Cesare was essential for a fast progress of our work. He is gratefully acknowledged for comments and assistance. We thank A. Fioretti for discussion to combine the geochemical point of view with our structural conception. We are highly indebted to R. Schönhofer and B. Schulz, who gave us an excellent introduction to the regional geology. Also, B. Schulz provided numerous structural maps of our working area. We thank W. Schnabel and the Geologische Bundesanstalt (Austria/Vienna) for granting access to the forestry roads of the Austrian part of the Rieserferner. G. Leitgeb (Antholz) and his colleagues kindly enabled the transport of the sample material in the field. Without their cableways the sampling might have been impossible. F. Heller and his colleagues (ETH Hönggerberg) made the HFA measurement available. They are highly acknowledged for discussion and assistance in the laboratory. Further we are in debt to J. Becker for the technical help at the Kappabridge. For detailed comments on a draft version of the manuscript Dr. R. Kruse is thankfully appreciated. Careful reviews by B. Henry and F. Hrouda helped to improve the paper.A. St. would like to thank the Niedersächsische Graduiertenförderung and the Deutscher Akademischer Austauschdienst for their scholarships and S. S. thanks the German Science Foundation for a Heisenberg-Fellowship (Si 438/10-1, 2).

References

Balsey, J.R., Buddington, A.F., 1960. Magnetic susceptibility anisotropy and fabric of some Adriondack granites and orthogneisses. American Journal of Science 258A, 6–20.

Bellieni, G., 1976. Contributo alla conscenza del plutone delle Vedrette di Ries (Alpe Orientali). Bollettino della Societa Geologica Italiana 95, 351–370.

Bellieni, G., 1978. Caratteri geochimici del massicco granodioritico tonalitico delle Vedrette die Ries (Rieserferner)-Alto Adige Orientale. Rendiconti della Societa Italiana di Mineralogia e Petrologia 34, 527–548.

Bellieni, G., 1980. The Cima di Villa (Zinsnock) massif: geochemical features and comparisons with the Vedrette di Ries (Rieserferner) pluton (Eastern Alps—Italy). Neues Jahrbuch für Mineralogie. Abhandlungen 138, 244–258.

Bellieni, G., Molin, G.M., Visona, D., 1979. The petrogenetic significance of garnets in the intrusive massifs of Bressanone and Vedrette di Ries (Eastern Alps—Italy). Neues Jahrbuch für Mineralogie. Abhandlungen 136, 238–253.

Bellieni, G., Peccerillo, A., Poli, G., 1981. The Vedrette di Ries (Rieserferner) Plutonic Complex: Petrological and geochemical data bearing on its genesis. Contributions to Mineralogy and Petrology 78, 145–156.

Bellieni, G., Peccerillo, A., Poli, G., Fioretti, A., 1984. The genesis of late Alpine plutonic bodies of Rensen and Monte Alto (Eastern Alps); inferences from major and trace element data. Neues Jahrbuch für Mineralogie. Abhandlungen 149, 209–224.

Bergmüller, F., Heller, F., 1996. The field dependence of magnetic anisotropy parameters derived from high-field torque measurements. Physics of the Earth and Planetary Interiors 96, 61–76.

Biermann, C., 1981. (100) deformation twins in naturally deformed amphiboles. Nature 292, 821–823.

Borsi, S., Del Moro, A., Sassi, F.P., Zirpoli, G., 1973. Metamorphic evolution of the austridic rocks to the south of Tauern Window (Eastern Alps). Radiometric and geo-petrologic data. Memorie della Societa Geologica Italiana 12, 549–571.

Borsi, S., Del Moro, A., Sassi, F.P., Zanferrari, A., Zirpoli, G., 1978. New petrologic and radiometric data on the alpine history of the austridic continental margin south of the Tauern Window (Eastern Alps). Memorie degli Istituti di Geologia e Mineralogia dell' Universita di Padova 32, 1–17.

Borsi, S., Del Moro, A., Sassi, F.P., Zirpoli, G., 1979. On the age of the Vedrette di Ries (Rieserferner) massif and its geodynamic significance. Geologische Rundschau 68, 41–60.

Bouchez, J.L., 1997. Granite is never isotropic: an introduction to AMS studies of granitic rocks. In: Bouchez, J.L., Hutton, D.W.H., Stephens, W.E. (Eds.). Granite: From Segragation of Melt to Emplacement Fabrics, Kluwer Academic, Dordrecht, pp. 95–112.

Bouchez, J.L., Gleizes, G., Djouadi, M.T., Rochette, P., 1990. Microstructure and magnetic susceptibility applied to the emplacement kinematics of granites: the example of the Foix pluton (French Pyrenees). Tectonophysics 184, 157–171.

Bouchez, J.L., Deal, C., Gleizes, G., Nedlec, A., Luney, M., 1992. Submagmatic microfractures in Granites. Geology 20, 35–38.

Brun, J.P., Gapais, D., Cogne, J.P., Ledru, P., Vigneress, J.L., 1990. The Flamanville Granite (Northwest France): an unequivocal example of a syntectonically expanding pluton. Geological Journal 25, 271–286.

Buddington, A.F., 1959. Granite emplacement with special reference to North America. Geological Society of America Bulletin 70, 671–747.

Cesare, B., 1992. Metamorfismo di contatto di rocce pelitiche nell' aureola di Vedrette di Ries (Alpi Orientali—Italia). Atti Ticinesi di Scienze della Terra 35, 1–7.

Coyle, D.A., 1994. The application of apatite fission track analysis to problems in tectonics. Unpublished Ph.D thesis. La Trobe University Bundoora, Victoria.

Daly, R.A., 1933. Igneous Rocks and the Depth of the Earth. McGraw-Hill, New York.

Dewey, J.F., 1988. Extensional collaps of orogens. Tectonics 7, 1123–1139.

Gleizes, G., Nédélec, A., Bouchez, J.L., Autran, A., Rochette, P., 1993. Magnetic susceptibility of the Mont-Louis Andorra Ilmenite-Type Granite (Pyrenees): A new tool for the petrographic characterisation and regional mapping of zone granite plutons. Journal of Geophysical Research, B. Solid Earth and Planets 98, 4317–4331.

Gleizes, G., Leblanc, D., Santana, V., Oliver, P., Bouchez, J.L., 1998. Sigmoidal structures featuring dextral shear during emplacement of the Hercynian granite complex of Cauterets-Panticosa (Pyrenees). Journal of Structural Geology 20, 1229–1245.

Grundmann, G., Morteani, G., 1985. The young uplift and thermal history of the central Eastern Alps (Austria/Italy), evidence from apatite fission track ages. Jahrbuch der Geologischen Bundesanstalt Wien 128, 197–216.

Heinisch, H., Sprenger, W., 1988. Mehrphasige Deformation und Pseudotachylitbildung im Gailtalkristallin und am Periadriatischen Lineament zwischen Sillian und Kötschach-Mauthen (Osttirol/Kärnten, Österreich). Erlanger Geologische Abhandlungen 116, 41–52.

Henry, B., 1975. Microteqtonique et anisotropie de susceptibilité et magnétique du massif tonalitique des Riesenferner-Vedrette di Ries (Frontiere Italo-Autrichienne). Tectonophysics 27, 155–165.

Hirth, G., Tullis, J., 1992. Dislocation creep regimes in quartz aggregates. Journal of Structural Geolology 14, 145–159.

Holder, M.T., 1979. An emplacement mechanism for post-kinematic granites and its implication for their geochemical features. In: Alderton, M.P., Tarney, J. (Eds.). Origin of Granite Batholiths: Geochemical Evidence, Shiva, Orpington, pp. 116–128.

Hrouda, F., 1982. Magnetic anisotropy of rocks and its application geology and geophysics. Geophysical Surveys 5, 37–82.

Hrouda, F., Lanza, R., 1989. Magnetic fabric in the Biella and Transversella stocks (Periadriatic Line): implications for the emplacement mode. Physics of the Earth and Planetary Interiors 56, 337–348.

Hutton, D.W.H., 1982. A tectonic model for the emplacement of the Main Donegal Granite, NW Ireland. Journal of the Geological Society of London 139, 615–631.

Hutton, D.W.H., 1988. Granite emplacement mechanisms and tectonic controls: inferences from deformation studies. Transactions of the Royal Society of Edinburgh: Earth Sciences 79, 245–255.

Hutton, D.W.H., Reavy, R.J., 1992. Strike-slip tectonics and granite petrogenesis. Tectonics 11, 960–967.

Jelinek, V., 1977. The statistical theory of measuring anisotropy of magnetic susceptibility of rock and its application. Geofyzika Brno, Czech Republik.

Jelinek, V., 1981. Characterisation of magnetic fabrics of rocks. Tectonophysic 79, 563–567.

John, B., Blundy, J.D., 1993. Emplacement-related deformation of granitoid magmas, southern Adamello massif, Italy. Geological Society of America Bulletin. 105, 1517–1541.

John, B., Stünitz, H., 1997. Magmatic fracturing and melt segaration during pluton emplacement: evidence from the Adamello massif (Italy). In: Bouchez, J.L., Hutton, D.W.H., Stephens, W.E. (Eds.). Granite: From Segragation of Melt to Emplacement Fabrics, Kluwer Academic, Dordrecht, pp. 55–74.

Kagami, H., Ulmer, P., Hansmann, W., Dietrich, V., Steiger, R.H., 1991. Nd–Sr isotopic and geochemical characteristics of the southern Adamello (northern Italy) intrusives: implications for crustal versus mantle origin. Journal of Geophysical Research 96, 14331–14346.

Kleinschrodt, R., 1978. Quartzkorngefügeanalyse im Altkristallin südlich des westlichen Tauernfensters. Erlanger Geologische Abhandlungen 114, 1–82.

Kruhl, J.H., 1996. Prism- and basal-plane parallel subgrain boundaries in quartz: a microstructural geothermobarometer. Journal of Metamorphic Geology 14, 581–589.

Laubscher, H.P., 1983. The late Alpine (Periadriatic) intrusions and the Insubric Line. Memorie della Societa Geologica Italiana 26, 21–30.

Mager, D., 1985. Geologische und petrographische Untersuchungen am Südrand des Rieserferner Plutons (Südtirol) unter Berücksichtigung des Intrusionsmechanismus. Unpublished Ph.D thesis. Universität Erlangen-Nürnberg.

Mainprice, D., Bouchez, J.L., Blumfeld, P., Tubia, J.M., 1986. Dominant c-slip in naturally deformed quartz: implications for drastic plastic softening at high temperatur. Geology 14, 819–822.

Mann, A., Scheuvens, D., 1998. Structural investigation of the northern contact of the Rieserferner Plutonic Complex (Eastern Alps)—first results, Terra Nostra. Schriften der Alfred Wegener Stiftung 98, 62.

Means, W.D., Park, Y., 1994. New experimental approach to understandig igneous texture. Geology 22, 323–326.

Paterson, S.R., Fowler, T.K., Schmidt, K.L., Yoshinobu, A.S., Yuan, E.S., Miller, R.B., 1998. Interpreting magmatic fabric patterns in plutons. Lithos 44, 53–82.

Pitcher, W.S., 1970. Ghost stratigraphy in granites: A review. In: G. Newhall, N. Rast (Eds.), Mechanisms of igneous intrusions, pp. 123–140, Special Issue of the Geological Journal 2.

Pitcher, W.S., Read, H.H., 1959. The main Donegal granite. Quarterly Journal of the Geological Society of London 114, 259–305.

Pitcher, W.S., Berger, A.R., 1972. The Geology of Donegal: A Study of the Granite Emplacement and Unroofing. Wiley Interscience, New York.

Ramsey, J.G., 1989. Emplacement kinematics of a granite diapir: the Chinamora batholith, Zimbabwe. Journal of Structural Geology 9, 191–209.

Ratschbacher, L., Frisch, W., Linzer, H.G., 1991. Laterat extrusion in the Eastern Alps, Part 2: structural analysis. Tectonics 10, 257–271.

Rochette, P., 1987. Magnetic susceptibility of the rock matrix related to magnetic fabric studies. Journal of Structural Geology 9, 1015–1020.

Rochette, P., Jackson, M., Aubourg, C., 1992. Rock magnetism and the interpretation of anisotropy of magnetic susceptibility. Reviews of Geophysics 30, 209–226.

Rosenberg, C.L., Berger, A., Schmid, S.M., 1995. Observations from the floor of a granitoid pluton: inferences on the driving force of final emplacement. Geology 23 (5), 443–446.

Saint Blanquat, M., Tikoff, B., 1997. Development of magmatic to solid-state fabrics during syntectonic emplacement of the Mono Creek Granite, Sierra Nevada Batholith. In: Bouchez, J.L., Hutton, D.W.H., Stephens, W.E. (Eds.). Granite: From Segragation of Melt to Emplacement Fabrics, Kluwer Academic, Dordrecht, pp. 231–252.

Sassi, F.P., Bellieni, G., Peccerillo, A., Poli, G., 1980. Some constraints on the geodynamic models in the Eastern Alps. Neues Jahrbuch für Geologie und Palaeontologie. Monatshefte 1980, 541–548.

Schmid, S., Aebli, H.R., Heller, F., Zingg, A., 1989. The role of the Periadriatic Line in the tectonic evolution of the Alps. In: Coward, M.P., Dietrich, D., Parks, R.G. (Eds.). Alpine Tectonics, Geological Society Special Publication 45, pp. 153–171.

Schönhofer, R., 1999. Das ostalpine Altkristallin der westlichen Lasörlinggruppe (Osttirol, Österreich): Kartierung, Stoffbestand und tektonometamorphe Entwicklung. Erlanger Geologische Abhandlungen 130, 1–128.

Schulz, B., 1989. Jungalpidische Gefügeentwicklung entlang der Defereggen-Antholz-Vals-Linie (Osttirol, Österreich). Jahrbuch der Geologischen Bundesanstalt Wien 132, 775–789.

Schulz, B., 1994. Geologische Karte des Altkristallins östlich des Tauferer Tals (Südtirol). Erlanger Geologische Abhandlungen 124, 1–28.

Siegesmund, S., Ullemeyer, K., Dahms, M., 1995. Control of magnetic rock fabrics by mica preferred orientation: a quantitative approach. Journal of Structural Geology 17, 1601–1613.

Siegesmund, S., Becker, J. 2000. The emplacement of the Ardara pluton (Ireland): New constraints from magnetic fabrics, rock fabrics and age dating. International Journal of Earth Sciences (in press).

Stacey, F.D., 1960. Magnetic anisotropy of igneous rocks. Journal of Geophysical Research 65, 2429–2442.

Steenken, A., Dahmen, O., Siegesmund, S., Heinrichs, T., 1999. Synectonic emplacement of the Rieserferner Pluton. Evidence from AMS and microstructures. Terra Abstracts 11, 682.

Stöckhert, B., 1982. Deformation und retrograde Metamorphose im Altkristallin südlich des westlichen Tauernfensters (Südtirol). Unpublished Ph.D thesis. Universität Erlangen-Nürnberg.

Stöckhert, B., 1984. K–Ar determinations on muscovites and phengites and the minimum age of the Old Alpine deformation in the Austridic basement south of the western Tauern Window (Ahrn valley, Southern Tyrol, Eastern Alps). Jahrbuch für Mineralogie Abhandlungen 150, 103–120.

Stöckhert, B., 1985. Pre-Alpine history of the Austridic basement to the south of the western Tauern Window (Southern Tyrol, Italy)—Caledonian versus Hercynian event. Neues Jahrbuch für Geologie und Palaeontologie. Monatshefte 10, 618–642.

Stöckhert, B., Brix, M.R., Kleinschrodt, R., Hurford, A.J., Wirth, R., 1999. Thermochronometry and microstructures of quartz—a comparison with experimental flow laws and predictions on the temperature of the brittle-plastic transition. Journal of Structural Geology 21, 351–369.

Tribe, I.R., D'Lemos, R.S., 1996. Significance of a hiatus in down-temperature fabric development within syntectonic quartz diorite complexes, Channel Islands, UK. Journal of the Geological Society of London 153 (1), 127–138.

von Blanckenburg, F., Davis, J.H., 1995. Slab breakoff: a model for syncollisional magmatism and tectonics in the Alps. Tectonics 14, 120–131.

von Blanckenburg, F., Davis, J.H., 1996. Feasibility of double slab breakoff (Cretaceous and Tertiary) during the Alpine convergence. Eclogae Geologicae Helvetiae 89, 111–127.